Separation Science and Technology
Publication details, including instructions for authors and subscription information:
http://www.informaworld.com/smpp/title~content=t713708471

Dynamic Characterization of Nanofiltration and Reverse Osmosis Membranes

Rémi E. Lebrun[a]; Yazhen Xu[a]
[a] DÉPARTEMENT DU GÉNIE CHIMIQUE, ÉCOLE D'INOÉNIERIE, UNIVERSITÉ DU QUÉBEC À TROIS-RIVIÈRES, TROIS-RIVIÈRES, QUEBEC, CANADA

To cite this Article Lebrun, Rémi E. and Xu, Yazhen(1999) 'Dynamic Characterization of Nanofiltration and Reverse Osmosis Membranes', Separation Science and Technology, 34: 8, 1629 — 1641
To link to this Article: DOI: 10.1080/01496399909353761
URL: http://dx.doi.org/10.1080/01496399909353761

SEPARATION SCIENCE AND TECHNOLOGY, **34**(8), pp. 1629–1641, 1999

Dynamic Characterization of Nanofiltration and Reverse Osmosis Membranes

RÉMI E. LEBRUN* and YAZHEN XU
DÉPARTEMENT DU GÉNIE CHIMIQUE
ÉCOLE D'INGÉNIERIE
UNIVERSITÉ DU QUÉBEC À TROIS-RIVIÈRES
C.P. 500, TROIS-RIVIÈRES, QUEBEC G9A 5H7, CANADA

ABSTRACT

An original method has been proposed to determine the dynamic permeability of membranes. Experiments were run under different operating conditions (various transmembrane pressures, membranes, concentrations, and solutes), and the experimental data were processed using this dynamic permeability model. The results show that permeability defined in this manner reflects the differences in the membrane behavior from pure water to a solution or from one solution to another. With dynamic permeability data, membrane condition can also be evaluated after use without the need to run experiments with pure water.

Key Words. Characterization; Dynamic; Membrane; Permeability; Nanofiltration; Reverse osmosis

INTRODUCTION

Membrane characterization is an indispensable step for membrane use in different fields. Many methods have been developed and applied at the microscopic scale for steric characterization (pore size and pore size distribution) (1, 2) and for ionic characterization (sign and charge strength) (3, 4). At the macroscopic scale, the determination of pure water permeability is a standardized characterization for all applications. Although the membrane is com-

* To whom correspondence should be addressed. E-mail: Remi_Lebrun@uqtr.uquebec.ca

pressed beforehand above the maximum operating pressure, the pure water permeability of membrane still varies with the applied pressure (5). In general, membrane permeability is derived from the mean value of a multiplicity of pure water permeability, which then is used to calculate or model the behavior during a solution separation. On one hand, the validity of pure water permeability is often questioned for solution separation, and on the other hand, the pure water permeability must be measured again to evaluate its state after use.

This study proposes an original method for determining the dynamic permeability of a membrane that clearly expresses the relationship between the permeate flux and the effective pressure gradient and which can evaluate the membrane condition after use without running pure water experiments.

THEORY AND METHOD

The process of nanofiltration/reverse osmosis is concurrently characterized by the permeate flux and the separation factor. The global separation factor and the intrinsic separation factor are defined respectively by the following expressions:

Global separation factor:

$$f = \frac{X_{A1} - X_{A3}}{X_{A1}} = 1 - \frac{X_{A3}}{X_{A1}} \tag{1}$$

Intrinsic separation factor:

$$f = \frac{X_{A2} - X_{A3}}{X_{A2}} = 1 - \frac{X_{A3}}{X_{A2}} \tag{2}$$

where X_{A1}, X_{A2}, and X_{A3} are the molar fraction of feed solution, concentrated boundary solution, and permeate solution, respectively.

Analysis of the nanofiltration/reverse osmosis process is generally based on the capillary flow model involving the viscous flow for the transport of Solvent B, which is proportional to the effective pressure gradient, the diffusion within the pores for the transport of Solute A, which is proportional to the effective concentration gradient, and the film theory which expresses the mass transfer effect on the high pressure side of the membrane on the total material transport across the membrane (6). This provides the following equations:

$$N_A = \frac{D_{AM}}{K\delta} \Delta C_{eff} = c \frac{D_{AM}}{K\delta} (X_{A2} - X_{A3}) \tag{3}$$

$$N_B = c \frac{A_i}{\mu} \Delta P_{eff} = c \frac{A_i}{\mu} [\Delta P - \Pi(X_{A2}) + \Pi(X_{A3})] \tag{4}$$

$$N = ck \ln\left(\frac{X_{A2} - X_{A3}}{X_{A1} - X_{A3}}\right) \tag{5}$$

where A_i = pure water intrinsic permeability of membrane (m)
ΔC_{eff} = effective molar concentration gradient (mol/m^3)
c = mean molar density (= 5.53×10^4 mol/m^3)
$D_{AM}/K\delta$ = solute transport parameter (m/s)
k = mass transfer coefficient on high pressure side of membrane (m/s)
N_A, N_B, N = molar flux of solute, solvent, and permeate, respectively (mol/m^2/s)
ΔP_{eff} = effective pressure gradient (Pa)
ΔP = transmembrane pressure (Pa)
μ = fluid viscosity (Pa·s)
$\Pi(X)$ = osmotic pressure of a solution with molar fraction X (Pa)

According to the definition, the relationship between N, N_A, and N_B is:

$$\left.\begin{aligned} N_A &= NX_{A3} \\ N_B &= N(1 - X_{A3}) \\ N &= N_A + N_B \end{aligned}\right\} \tag{6}$$

Since the volume flux is equal to the molar flux divided by the molar density ($J = N/c$), three equations are then derived to calculate the volume permeate flux:

$$J = \left(\frac{D_{AM}}{K\delta}\right)\left(\frac{X_{A2} - X_{A3}}{X_{A3}}\right) \tag{7}$$

$$J = \frac{(A_i/\mu)[\Delta P - \Pi(X_{A2}) + \Pi(X_{A3})]}{1 - X_{A3}} \tag{8}$$

$$J = k \ln\left(\frac{X_{A2} - X_{A3}}{X_{A1} - X_{A3}}\right) \tag{9}$$

where J is the volume permeate flux across the membrane (m^3/m^2/s).

The following formula is obtained from Eq. (8) to calculate the osmotic pressure gradient $\Delta\Pi$:

$$\Delta\Pi = \Pi(X_{A2}) - \Pi(X_{A3}) = \Delta P - \mu J(1 - X_{A3})/A_i \tag{10}$$

On one hand, once the permeate flux J and molar fraction of solute in the permeate X_{A3} are measured by experimentation, the osmotic pressure gradient can be calculated by Eq. (10). On the other hand, Robinson and Stokes's equation (7) shows the relationship between the osmotic pressure and the concen-

tration of solute. So, the concentration of the concentrated boundary solution X_{A2} can be determined. In practice, however, Expression (10) is often a poor description of reality due to the uncertainty of the value of A_i (measured with pure water). In some cases it gives a value of $\Pi(X_{A2})$ smaller than that of $\Pi(X_{A1})$. Hence, another method will be used to determine the coefficient between the permeate flux and the effective pressure gradient.

Knowing that the permeate flux J is proportional to the effective pressure gradient ΔP_{eff}, A_{id} is used as a coefficient between J and ΔP_{eff}, to distinguish it from A_i, in which

$$J = \frac{A_{id}}{\mu} \Delta P_{eff} \qquad \text{or} \qquad \mu J = A_{id} \Delta P_{eff} \tag{11}$$

where A_{id} is the dynamic solution permeability of membrane (m).

At first it was not possible to calculate the effective pressure gradient ΔP_{eff} due to the unknown solute concentration in the boundary layer X_{A2}. Hence the apparent pressure gradient ΔP_a is defined as

$$\Delta P_a = \Delta P - \Pi(X_{A1}) + \Pi(X_{A3}) \tag{12}$$

When X_{A2} tends toward X_{A1}, there is no concentration polarization layer, whereas $\Delta P_{eff} = \Delta P_a$. Hence the following equation is correct:

$$\mu J = A_{id} \Delta P_a \qquad \text{when } X_{A2} \rightarrow X_{A1} \tag{13}$$

Moreover, when ΔP_a tends toward zero, there is also no concentration polarization layer. So the value of A_{id} can be determined as follows:

$$A_{id} = \left. \frac{\mu J}{\Delta P_a} \right|_{X_{A2} \rightarrow X_{A1}} \tag{14}$$

or

$$A_{id} = \left. \frac{d(\mu J)}{d(\Delta P_a)} \right|_{\Delta P_a \rightarrow 0} \tag{15}$$

EQUIPMENT AND PROTOCOL

The equipment used in this study has been described by Kusberg et al. (8). This device is designed to test up to 12 membrane samples, each measuring 1.2×10^{-3} m^2. Each piece is kept in a cell with a very narrow pipe. This apparatus is schematically portrayed in Fig. 1. Three sensors were installed to measure the process variables (pressure, flow, and temperature). The permeate flux was measured by weight, while the solution and permeate concentrations were determined through a conductivity meter. A pre-filter (Gelman Sciences) of 0.1 μm was installed upstream of the pure water reservoir.

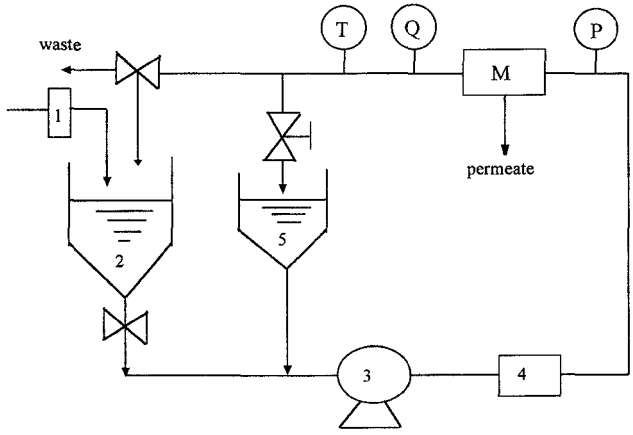

1- pre-filter
2- water reservoir
3- pump
4- thermostat
5- solution reservoir
P- pressure sensor
T- temperature sensor
Q- flow sensor
M- membrane cell

FIG. 1 Schematic experimental representation.

The solutions used in the study were prepared with this pure water. The water permeability of each membrane was measured before and after use. At an operating pressure of 2.76 MPa, the load is 0.13 MPa, measured manually with a manometer, which represents approximately 5% of the operating pressure.

Tests were run on six types of commercial membranes and four types of cellulose acetate membranes manufactured in-house. The commercial membranes were supplied by two companies, and can be grouped into two categories: nanofiltration membranes and reverse osmosis membranes. The four types of cellulose acetate membrane are: membrane with no heat treatment and membranes with 60, 70, and 80°C treatment for 1 hour respectively. Sodium chloride and sodium sulfate solutions were used for the experiments, which were run under different transmembrane pressures and different solution concentrations. The membranes and experiment protocol used are summarized in Table 1.

TABLE 1
Summary of Membranes Used and the Protocol

Type	Membrane Name	Membrane Made by	Solution NaCl (ppm)	Solution Na_2SO_4 (ppm)	Pressure (MPa)
Nanofiltration	BQ01	Osmonics	10,000	—	0.69–1.38–2.07–2.76–3.45
			7,000	7,000	1.38–2.07–2.76
	NF45	Filmtec	10,000	—	0.69–1.38–2.07–2.76–3.45
			7,000	7,000	
Reverse osmosis	MX07	Osmonics			
	ST10	Osmonics	7,000	7,000	1.38–2.07–2.76
	MS10	Osmonics			
	SW30	Filmtec			
Reverse osmosis (cellulose acetate)	None 60°C 70°C 80°C	In-house	3,500	—	1.38–2.07–2.76–3.45

RESULTS AND DISCUSSION

Determination of A_{id}

The relationship between (μJ) and ΔP_a can be simulated from the experimental data; the function of the simulation $\mu J = f(\Delta P_a)$ with the constraint of $J = 0$ when $\Delta P_a = 0$ would be a second- or third-order polynomial according to the number of experimental points. According to Eq. (15), the value of the dynamic solution permeability A_{id} is determined by the derivation of μJ with respect to ΔP_a when $\Delta P_a = 0$. This is the value of the coefficient of the first-degree term of the polynomial. Figure 2 illustrates how to determine the value of A_{id}.

Transmembrane Pressure Effect

The pressure gradient is the driving force for solvent transport across the membrane. Because of the presence of the concentration polarization phenomenon, the increased transmembrane pressure is not always worthwhile. However, the concentration polarization phenomenon is difficult to observe experimentally as a function of the operating conditions, and a number of models of varying complexity have been proposed (9, 10). The dynamic permeability model presented in this study can be used to evaluate this phenomenon as a function of operating conditions.

Once the value of A_{id} is determined, it will be used instead of A_i in Eq. (10) to calculate the osmotic pressure on the above side of the membrane $\Pi(X_{A2})$. Finally, we can calculate the molar fraction of solute in the boundary layer X_{A2}. Figure 3 represents the evolution of X_{A2}/X_{A1} versus the transmembrane pressure. We have seen that the polarization concentration rate (X_{A2}/X_{A1}) increases rapidly as the transmembrane pressure rises. This indicates that when the concentration polarization becomes significant, the increased transmembrane pressure is no longer worthwhile for the process.

Concentration Effect

The concentration gradient is the driving force for solute transport across the membrane. In order to determine the concentration effect, we have calculated the value of the dynamic solution permeability of Membrane NF45 with NaCl at two different concentrations. The calculated result showed that the dynamic permeability value decreases when the concentration rises. This indicates that the dynamic permeability can vary with the feed concentration. A detailed investigation of this phenomenon is under way and will be reported in a full paper in due course.

Effect of Membrane Type

As the membrane is at the core of the process, the efficiency of separation varies from one membrane to another. This is due to powerful solute–membrane interactions resulting from the charge usually carried by these mem-

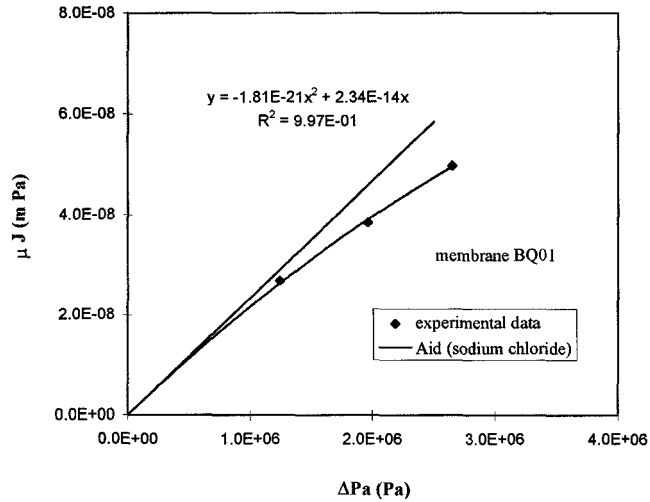

FIG. 2 Determination of the dynamic solution permeability of Membrane BQ01 with NaCl.

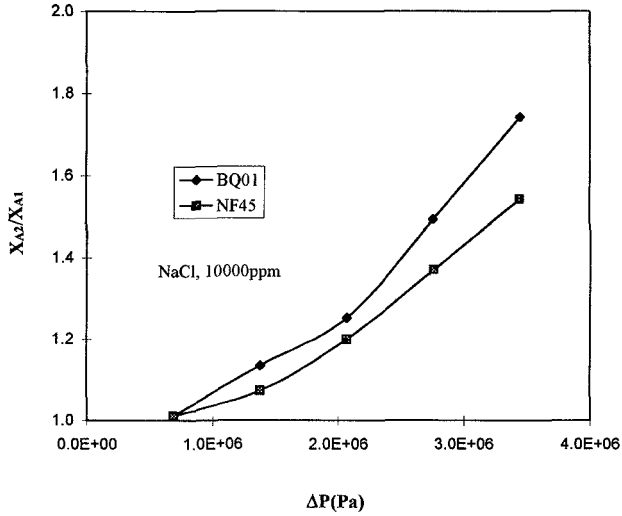

FIG. 3 Effect of transmembrane pressure on the concentration polarization rate (X_{A2}/X_{A1}) for Membranes BQ01 and NF45.

branes and from the small pore dimensions. The dynamic permeability and intrinsic separation factor of six commercial membranes were compared for NaCl and Na_2SO_4 solutions of 7000 ppm ($X_{A1} = 2.15 \times 10^{-3}$ for NaCl, $X_{A1} = 0.886 \times 10^{-3}$ for Na_2SO_4). Figure 4 shows that the nanofiltration membranes (BQ01 and NF45) have a superior dynamic permeability both for NaCl and for Na_2SO_4. Figure 5 shows that the value of the intrinsic separation factor for the Na_2SO_4 solution is so close to 1 that no difference is observed between the membranes. Since the nanofiltration membranes give a superior permeability and a retention of Na_2SO_4 as high as reverse osmosis membranes, nanofiltration membranes will be a good choice for Na_2SO_4 separation. For the NaCl solution, the intrinsic separation factor varied between 40 and 99% depending on the membrane type. The nanofiltration membranes show a lower salt retention. The highest salt retention is seen with Membranes MS10 and SW30.

Effect of Solute

When a solute nears the membrane surface, it succumbs to different interaction forces. In the case of charged compounds (salts), the contributing phenomena are more complex because there is competition between different phenomena such as steric hindrance, electric interactions and, in some cases, a concentration polarization layer. As shown in Fig. 5, the intrinsic separation

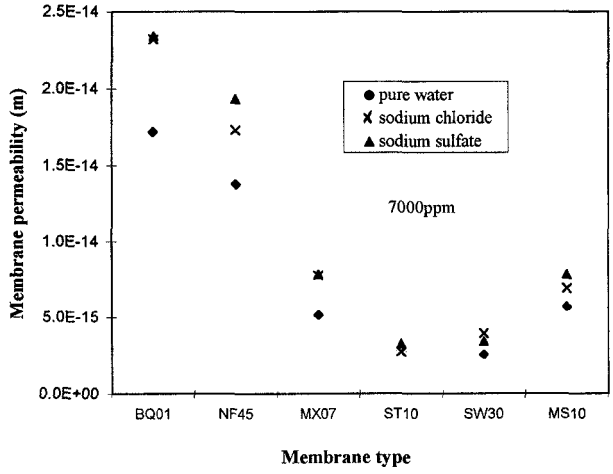

FIG. 4 Effect of membrane type on the dynamic solution permeability for NaCl and Na_2SO_4 solutions.

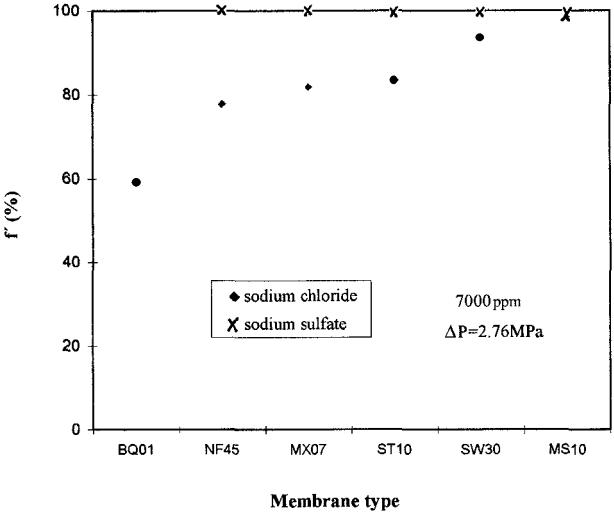

FIG. 5 Effect of membrane type on the intrinsic separation factor for NaCl and Na_2SO_4 solutions.

factor for the Na_2SO_4 solution reached 99% for the entire group of membranes, whereas for the NaCl solution it varied between 40 and 99% depending on the membrane type. The fact that the membranes retained more Na_2SO_4 than NaCl can be explained by the combined steric exclusion (Stokes' radius for NaCl = 1.52×10^{-10} m and Stokes' radius for Na_2SO_4 = 1.99×10^{-10} m) and electric repulsion between the solutes and the membranes. As to the dynamic permeability, Fig. 4 shows that the dynamic solution permeability is greater than the pure water permeability for both NaCl and Na_2SO_4. The fact that the membrane permeation rate in the presence of electrolyte solute in the feed may increase significantly from that in the absence of electrolyte solute has been reported by other authors (11). Depending on the membrane type, the dynamic permeability for NaCl can be slightly greater or less than that for Na_2SO_4.

Effect of Membrane Heat Treatment

The heat treatment consists of modifying the porous structure of the membrane by shrinking the pore size, and the temperature determines the structural modification (12). As a result of pore size shrinkage, the permeate flux drops and the intrinsic separation factor rises in relation to the degree of heat treatment (13). In our study the effect of heat treatment on pure water permeability and on dynamic solution permeability were compared. Figure 6 shows that

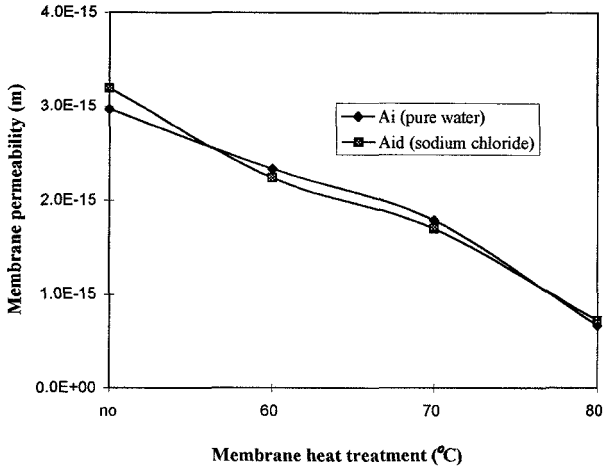

FIG. 6 Comparison of the effect of heat treatment of cellulose acetate membrane on the pure water permeability and the dynamic solution permeability.

evolution of dynamic solution permeability as a function of heat treatment is similar to that of pure water permeability. However, depending on the degree of heat treatment, the value of dynamic solution permeability can be greater or less than that of pure water permeability.

CONCLUSION

In this study we have proposed an original method to determine the dynamic permeability of a membrane. This dynamic solution permeability reflects the differences in membrane behavior from pure water to a solution or from one solution to another. The nanofiltration/reverse osmosis process can be analyzed in a rigorous yet user-friendly manner, and the condition of the membrane after use can be evaluated using dynamic permeability data without the need to run pure water experiments.

For the same membrane, when the solution to be filtered is different, the dynamic permeability value is not the same, which means that the membrane does not react in the same manner from one solution to another. Classic water permeability cannot reflect these differences in membrane behavior.

Parameters which cannot be measured, such as the concentration upstream of the membrane in the boundary layer X_{A2}, can be calculated from dynamic permeability values A_{id}, from which the intrinsic separation factor f' is then calculated.

The concentration polarization phenomenon is difficult to observe experimentally as a function of the operating conditions. The dynamic permeability model presented in this study can be used to evaluate this phenomenon as a function of operating conditions. This could have considerable significance in research strategies of optimal operating conditions.

NOMENCLATURE

A_i	pure water intrinsic permeability of membrane (m)
A_{id}	dynamic solution permeability of membrane (m)
c	mean molar density, $c = 5.53 \times 10^4$ mol/m^3
C	molar concentration (mol/m^3)
$D_{AM}/K\delta$	solute transport parameter (m/s)
f, f'	global and intrinsic separation factors, respectively
J	volume permeate flux (m^3/m^2/s)
k	mass transfer coefficient on high pressure side of membrane (m/s)
N	molar permeate flux (mol/m^2/s)
P	pressure (Pa)
X	molar fraction

Greek Letters

Δ	gradient
μ	fluid viscosity (Pa·s)
Π	osmotic pressure (Pa)

Subscripts

A	solute
B	solvent
M	membrane
a	apparent value
eff	effective value
i	intrinsic
1	within the solution
2	upstream of the membrane in the boundary layer
3	downstream of the membrane

ACKNOWLEDGMENTS

We thank Hydro-Québec for its financial support for the publication of this article. Our thanks also go to the CNRC of Ottawa for its financial participation in some experiments, and to the Hayka Company for automation development, data sampling, and the provision of the experimental rigs. Thanks also are due to Didier J. Kusberg and Gaétanne Boulanger for running some experiments, and to Nengyou Jia for producing and running experiments with cellulose acetate membranes.

REFERENCES

1. K. Chan, T. Matsuura, and S. Sourirajan, "Interfacial Forces, Average Pore Size and Pore Size Distribution of Ultrafiltration Membranes," *Ind. Eng. Chem., Prod. Res. Dev., 21*(4), 605–612 (1982).
2. P. Dietz, K. Hansma, O. Inacker, H.-D. Lehmann, and K.-H. Herrmann, "Surface Pore Structures of Micro- and Ultrafiltration Membranes Imaged with the Atomic Force Microscope," *J. Membr. Sci., 65*, 101–111 (1992).
3. M. Nystrom, M. Linstrom, and E. Matthiasson, "Streaming Potentials as a Tool in the Characterization of Ultrafiltration Membranes," *Colloids Surf., 36*, 297–312 (1989).
4. T. Courtois, *Caractérisation des membranes de nanofiltration*, Presented at 1st Nanofiltration & Applicatinon Workshop France-Canada, Trois-Rivières, Quebec, Canada, June 2–4, 1997.
5. Y. Xu, R. E. Lebrun, P.-J. Gallo, and P. Blond, "Treatment of Textile Dye Plant Effluent by Nanofiltration Membrane," Submitted, 1999.
6. S. Sourirajan and T. Matsuura, *Reverse Osmosis/Ultrafiltration Principles*, Division of Chemistry, National Research Council Canada, Ottawa, Canada, 1985.

7. R. A. Robinson and R. H. Stokes, *Electrolyte Solutions*, 2nd ed., Butterworths, London, 1959.
8. D. J. Kusberg, R. E. Lebrun, and A. Kumar, "Characterization of Reverse Osmosis and Nanofiltration Membranes by an Automated System," *Can. J. Chem. Eng.*, *74*(12), 896–904 (1996).
9. C. R. Bouchard, P. J. Carreau, T. Matsuura, and S. Sourirajan, "Modeling of Ultrafiltration: Prediction of Concentration Polarization Effects," *J. Membr. Sci.*, *97*, 215–229 (1994).
10. D. R. Trettin and M. R. Doshi, "Limiting Flux in Ultrafiltration of Macromolecular Solutions," *Chem. Eng. Commun.*, *4*, 507–522 (1980).
11. A. Hamza, G. Chowdhury, T. Matsuura, and S. Sourirajan, "Study of Reverse Osmosis Separation and Permeation Rate for Sulfonated Poly(2,6-dimethyl-1,4-phenylene Oxide) Membranes of Different Ion Exchange Capacities," *J. Appl. Polym. Sci.*, *58*, 613–620 (1995).
12. R. E. Lebrun, "Porométrie des membranes d'osmose reverse en acétate de cellulose: Influence de la préparation et modélisation," Ph.D. Thesis, École Polytechnique, Montréal, 1990.
13. Y. Wang, W. W. Y. Lau, and S. Sourirajan, "Effects of Pretreatments on Morphology and Performance of Cellulose Acetate (formamide type) Membranes," *Desalination*, *95*, 155–169 (1994).

Received by editor May 26, 1998
Revision received September 1998